Wireless Pers Commun (2012) 64:233–253
DOI 10.1007/s11277-010-0183-5

On the Performance of Energy-Division Multiple Access with Regular Constellations

Pierluigi Salvo Rossi · Gianmarco Romano · Francesco Palmieri

Published online: 21 November 2010

Abstract In this paper we describe a multiple-access protocol in which different users are assumed to share the same bandwidth and the same pulse. Users employ the same modulation (binary-phase shift keying, quadrature-phase shift keying, and rectangular-phase shift keying are considered) with different transmitted magnitude, and are discriminated on the basis of the corresponding magnitude at receiver location. Conditions for user discrimination are analyzed. The proposed receiver uses successive decoding in order to avoid exponential complexity of maximum-likelihood decoding. Such a scheme, compared to orthogonal multiaccess schemes (e.g. time- or frequency-division multiple access) allows to achieve larger normalized throughput for systems operating in large signal-to-noise ratio range, and may be jointly applied with classical protocols in personal-area networks. Analytical and numerical results, in terms of bit error rate and normalized throughput, are derived for performance evaluation on additive white Gaussian noise channels.

Keywords Amplitude modulation · Bit error rate · Multiple access · Normalized throughput · Successive decoding

1 Introduction

Classical multiple access systems for communication are based on time, frequency or code division. Their advantages and disadvantages have been discussed in the classical literature

P. Salvo Rossi (✉) · G. Romano · F. Palmieri
Department of Information Engineering, Second University of Naples, Via Roma 29,
81031 Aversa, CE, Italy
e-mail: pierluigi.salvorossi@unina2.it

G. Romano
e-mail: gianmarco.romano@unina2.it

F. Palmieri
e-mail: francesco.palmieri@unina2.it

[1–4]. The increasing demand of bandwidth in modern applications requires to consider scenarios in which resources allocable with the classical schemes have been saturated. In such cases, several users may need to use simultaneously the same bandwidth with the same baseband pulse and still be able to get multiple access at the receiver. Moreover, in personal-area networks and sensor networks, the infrastructure availability is often not known *a priori* and simple access schemes are desirable.

Bandwidth-Efficient Multiple Access (BEMA) was recently introduced [5,6] as a technique to achieve minimum spectral occupancy with given Quality-of-Service constraints usually expressed in terms of power limitations. BEMA framework includes Time-Division Multiple Access (TDMA) and Frequency Division Multiple Access (FDMA) at one hand, and Identical Waveform Multiple Access (IWMA) at the other hand, as special cases. In [7], signal design and power control are combined for multiuser linear receivers: the goal is the minimization of the processing gain (i.e. the spectral occupancy) while guaranteeing given Quality-of-Service constraints in terms of Signal-to-Interference Ratio (SIR). Such an approach differs from BEMA, as compared in [8], as it focuses on sum capacity maximization (while BEMA focuses on a set of QoS) and also employs a linear receiver (while BEMA employs a decision-feedback receiver).

Tested on different scenarios with several power disparities and both symmetric and asymmetric SIR constraints, BEMA has shown to be superior to the other techniques. This paper explores a complementary problem: the spectral occupancy is fixed (we only consider one-dimensional and two-dimensional modulations), while power allocation is exploited to allow simultaneous transmissions among users. More specifically, we explore a multiple access scheme that allows several users to transmit simultaneously with the same baseband pulse according to one of the following formats: binary phase-shift keying (BPSK), quadrature-phase shift keying (QPSK), rectangular-phase shift keying[1] (RPSK). The receiver sees a structured multi-user constellation, and the information transmitted by each user is recovered exploiting the differences in the received energy from each user. Such a system, here called Energy-Division Multiple Access (EDMA) and IWMA in [5,6], essentially manages multiple access via a slight generalization of the power control procedures [9,10]. From the receiver point of view, the resulting EDMA constellation is equivalent to single *pulse amplitude modulation* (PAM) signaling (resp. *quadrature amplitude modulation* (QAM) signaling) if the single user employs BPSK (resp. QPSK or RPSK), but such a constellation is obtained as a superposition of several single-user constellations. The presence of a multiuser scenario imposes appropriate constraints to make the receiver problem solvable. EDMA may also be viewed as a technique for Trellis Coded Multiple Access (TCMA) [11], since superposition is used to build one equivalent multi-user constellation from single-user constellations. TCMA is used in order to obtain non-equiprobable constellation and approach channel capacity [12], with various design criteria provided in [13].

Preliminary results for the average performance of BPSK-EDMA has been discussed in [14,15]. In this paper, bit error rate (BER) vs. signal-to-noise ratio (SNR) curves for uncoded transmissions over an additive white Gaussian channel (AWGN) are analytically derived (also confirmed by computer simulations) and compared for BPSK-EDMA, QPSK-EDMA, and RPSK-EDMA. More specifically, the contributions of this paper are: (i) to find the condition such that EDMA is possible with simple reception, i.e. using successive decoding thus avoiding Maximum Likelihood (ML) decoding; (ii) to provide analytic expression for the performance of EDMA in terms of BER for each single user as well as the average performance of the whole system; (iii) to compute numerically the average performance of

[1] It will be better defined in Sect. 2.

EDMA in terms of normalized throughput of the system. The rest of the paper is organized as follows: Sect. 2 presents the system model; the analytical conditions that make EDMA feasible are described in Sect. 3; in Sect. 4 the average and the single-user performance are derived analytically; Sect. 5 compares and comments the performance of different system configurations; some concluding remarks are given in Sect. 6.

Notation - upper-case bold letters denote matrices with $A_{n,m}$ denoting the (n, m)th entry of $\boldsymbol{A}$; lower-case bold letters denote column vectors with a_n denoting the nth entry of $\boldsymbol{a}$; $\Re(a)$ and $\Im(a)$ denote the real and the imaginary parts of a, respectively; $|a|$ denote the absolute value of a; j denotes the imaginary unit; $\mathbf{1}_N$ and $\mathbf{0}_N$ denote column vectors of length N whose entries are 1 and 0, respectively; $\boldsymbol{I}_N$ denotes the identity matrix of order N; $\boldsymbol{I}_N^{(\mathrm{a})}$ denotes the anti-identity matrix of order N; $(.)^T$ denotes the transpose operator; $\otimes$ denotes the Kronecker product; $\mathrm{diag}(\boldsymbol{A}, n)$ denotes a column vector containing elements from the nth diagonal of $\boldsymbol{A}$ with $n = -(N-1), \ldots, 0, 1, \ldots, (N-1)$ for $N \times N$ matrices (e.g. $\mathrm{diag}(\boldsymbol{A}, 0)$ is the main diagonal); $\mathcal{N}(\mu, \sigma^2)$ denotes a normal distribution with mean μ and variance σ^2; $\mathcal{N}_{\mathbb{C}}(\boldsymbol{\mu}, \boldsymbol{\Sigma})$ denotes a circular symmetric complex normal distribution with mean vector $\boldsymbol{\mu}$ and covariance matrix $\boldsymbol{\Sigma}$; the symbol $\sim$ means "distributed as"; calligraphic letters denote subsets with $|\mathcal{A}|$ denoting the cardinality of $\mathcal{A}$; $\times$ denotes the cartesian product between sets.

2 System Model

We consider a set of N users transmitting to a single receiver over a multiple-access channel using simultaneously the same pulse. With multiple-access channel we mean the possibility to implement a multiple-input single-output channel where the multiple inputs refer to different users, as shown in Fig. 1. Although our approach can be applied to more sophisticated scenarios, we focus here, for sake of clarity, on the simplest case in which users transmissions are assumed synchronous at the receiver. It is worth noticing that synchronism is feasible (having the same requirements as for TDMA), more details on synchronization techniques may be found in [16]. The analysis of synchronization errors and their effects are beyond the scope of this paper.

The baseband discrete-time signal, after matched filtering and sampling at the symbol rate, is written as

$$y = \sum_{n=1}^{N} g_n x_n + w = \boldsymbol{g}^T \boldsymbol{x} + w \ , \tag{1}$$

where $w \sim \mathcal{N}(0, \sigma^2)$ is the overall additive noise, x_n and g_n are the modulated symbol of the nth user and the corresponding gain at the receiver, $\boldsymbol{x} = (x_1, \ldots, x_N)^T$ is the *transmission vector*, and $\boldsymbol{g} = (g_1, \ldots, g_N)^T$ is the *gain vector*. Each gain should be expressed as $g_n = h_n\sqrt{\mathcal{E}_n}$, i.e. depending on $\mathcal{E}_n$ and h_n, denoting respectively the transmitted energy per

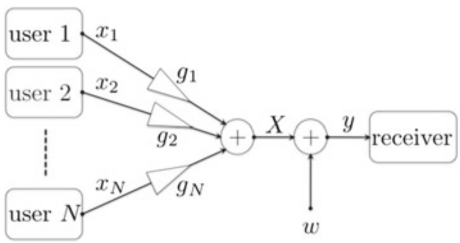

Fig. 1 Multiple-access channel with N users

bit and the channel coefficient experienced by the nth user. However, throughout the paper we limit our analysis to the AWGN channel, i.e. $h_n = 1$ and $g_n \in \mathbb{R}$, that allows to study the fundamental properties of the model, leaving the extension to fading channels to future work. Also we define the average energy per bit spent on each channel use as

$$\mathcal{E}_{\text{av}} = \frac{1}{N}\sum_{n=1}^{N}\mathcal{E}_n \ ,$$

while the user SNR and the average SNR are defined respectively as

$$\Gamma_n = \frac{\mathcal{E}_n}{2\sigma^2} \ , \qquad \Gamma_{\text{av}} = \frac{\mathcal{E}_{\text{av}}}{2\sigma^2} \ .$$

We consider the case of uncoded transmission with BPSK and QPSK modulation for the single user. In the BPSK case a single bit b_n is mapped into the transmitted symbol $x_n = 2b_n - 1$; in the QPSK case a pair of bits (b_n', b_n'') is mapped into the transmitted symbol $x_n = (2b_n' - 1) + j(2b_n'' - 1)$. As bits and symbols are mapped to each other biunivocally, we will often confuse them in the following. BPSK-EDMA refers to the case in which $x_n \in \{\pm 1\}$ and $\mathcal{E}_n = g_n^2$. QPSK-EDMA refers to the case in which $x_n \in \{\pm 1 \pm j\}$ and $\mathcal{E}_n = g_n^2$, i.e. each user uses the same BPSK modulation on both *in-phase* and *quadrature* components. Finally, we consider the case in which each user uses two different BPSK modulations on *in-phase* and *quadrature* components, respectively with gains $g_n^{(I)}$ and $g_n^{(Q)}$, denoted Rectangular Phase Shift Keying (RPSK). Mapping between bits and symbols is the same as for QPSK, thus RPSK-EDMA refers to the case in which $x_n \in \{\pm 1 \pm j\}$ and $\mathcal{E}_n = ((g_n^{(I)})^2 + (g_n^{(Q)})^2)/2$, while the model in Eq. (1) is replaced with

$$y = \sum_{n=1}^{N}\left(g_n^{(I)}\Re(x_n) + jg_n^{(Q)}\Im(x_n)\right) + w \ . \tag{2}$$

It is worth noticing that QPSK-EDMA matches both the models in Eqs. (1) and (2) with $g_n = g_n^{(I)} = g_n^{(Q)}$.

The problem of recovering $\boldsymbol{x}$ from the scalar y appears though, since users transmit at same time, on the same band and with same code, i.e. a degenerate overloaded CDMA system [17,18]. However, the contributions from different users can in fact be discriminated on the basis of their energy because if users are at different distances from the receiver, they should be naturally differentiable on the basis of their received magnitude. Although it may appear that the system employs a classical 2^N-ary linear modulation scheme, the novel point of view is that the generic symbol of the constellation at the receiver is built upon contributions from different users, each acting on a different digit depending on the corresponding energy. The structure of the decision-feedback receiver considered for BPSK-EDMA is shown in Fig. 2, where $\hat{x_n}$ denotes the estimate for the symbol x_n. The properties of the gain vector $\boldsymbol{g}$ to make reception feasible are studied in the next section. The structure of the receiver for QPSK-EDMA and RPSK-EDMA is obtained straightforward.

3 Separability

First we consider that each user adopts BPSK modulation, i.e. $x_n \in \{\pm 1\}$. The 2^N configurations of $\boldsymbol{x}$ constitute the 2^N-ary equivalent PAM constellation, $X = \boldsymbol{g}^T\boldsymbol{x} \in \{s_1, \ldots, s_{2^N}\}$. Figure 3 shows the case for $N = 3$. The association of the scalar value y to a constellation point is feasible if there is a one-to-one mapping between X and $\boldsymbol{x}$, i.e. no pair of

Fig. 2 Decision-feedback receiver for BPSK-EDMA

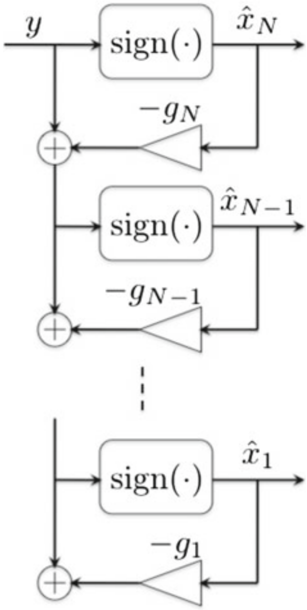

bit configurations can correspond to the same constellation point. It is easy to show the equivalence of such property with the following *Separability Condition*

$$\sum_{n=1}^{N} v_n g_n \neq 0 \ , \tag{3}$$

for each combination with $v_n \in \{-1, 0, +1\}$ except the one with all null coefficients [19]. The separability condition means that two different symbol configurations (i.e. bit configurations) $\boldsymbol{x}_i$ and $\boldsymbol{x}_j$ must correspond to two different constellation points s_i and s_j. Even if such a condition is satisfied, the constellation points may still be very confused on the observation axis, and the association of the constellation point to users bits may be somewhat cumbersome. Assuming, without loss of generality, that gains are ranked as $0 < g_1 < \cdots < g_N$, a sufficient condition to satisfy separability for all users is

$$g_n > \sum_{m=1}^{n-1} g_m \qquad n = 2, \ldots, N. \tag{4}$$

Such a constraint allows conditional separability of each user on the decision taken on the previous ones: users may be decoded with a successive cancellation scheme going from user N to user 1. In such case, successive cancellation scheme is the optimum decoding strategy. Equation (4) as sufficient condition for separability has been previously derived within an overloaded CDMA scenario [18] and also discussed in [14, 15]. Also, it guarantees asymptotic (for noise variance going to 0) vanishing BER for all users [20].

Since asymptotic BER depends essentially on the minimum distance among constellation points, users can share similar asymptotic performances if the overall PAM constellation is constrained to be uniform. Regularly-spaced overall PAM constellation is obtained if

$$g_n = \frac{d}{4} 2^n, \tag{5}$$

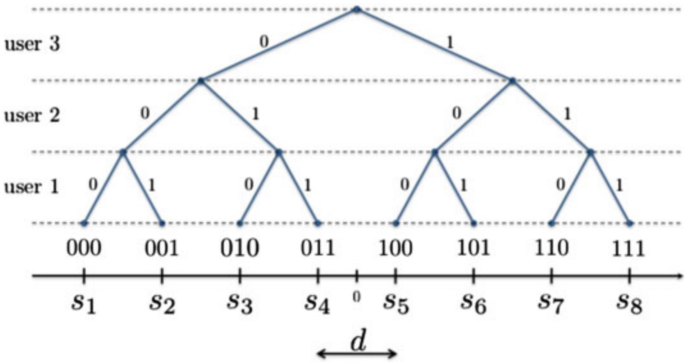

Fig. 3 Tree structure for a BPSK-EDMA system with 3 users

where d denotes the distance between two adjacent symbols in the PAM constellation. Note that no Gray coding is allowed because the code is imposed by the linear mapping as shown in Fig. 3. The extension to two-dimensional modulation is straightforward, and regularly QAM is obtained if

$$g_n^{(I)} = \frac{d}{4}2^n \ , \qquad g_n^{(Q)} = \frac{d}{4}2^n \ ,$$

representing the QPSK-EDMA case, in which both the in-phase and quadrature components follows the same ordering with the user index n, or if

$$g_n^{(I)} = \frac{d}{4}2^n \ , \qquad g_n^{(Q)} = \frac{d}{4}2^{N-n+1} \ ,$$

representing the RPSK-QPSK case, in which the in-phase and quadrature components follows a reversed ordering with the user index n. It is worth noticing that the RPSK-EDMA, due to the reversed ordering of the two components, reduces the difference among the requested energy per user, thus improving the fairness of the system.

4 Performance Analysis

System performance will be evaluated in terms of average-user BER and single-user BER, in the following denoted as $P_{e,\text{av}}$ and $P_e(n)$, respectively. The former accounts for the error rate on the user bits averaging the behavior of all the users in the systems, the latter accounts for the error rate on the user bits of a specific user. Average-user BER is related to single-user BER via $P_{e,\text{av}} = (1/N)\sum_{n=1}^{N} P_e(n)$, or alternatively may be directly computed as the ratio between the average number of bits in error over the number of transmitted bits.

Average-user BER will be evaluated with respect to (w.r.t.) average SNR, while single-user BER will be evaluated w.r.t. both average SNR and user SNR. In the BPSK-EDMA case, from Eq. (5), average SNR and user SNR are computed respectively as

$$\Gamma_{\text{av}} = \frac{2^{2N}-1}{12N}\frac{d^2}{2\sigma^2} \ , \qquad \Gamma_n = \frac{3N2^{2(n-1)}}{2^{2N}-1}\Gamma_{\text{av}} \ . \tag{6}$$

In the QPSK-EDMA, each user transmits two bits with double energy per channel use w.r.t. the BPSK-EDMA, thus average SNR and user SNR are the same as in Eq. (6). In the RPSK-EDMA case, average SNR is the same as for QPSK-EDMA, expressed by Eq. (6), while user

SNR is

$$\Gamma_n = \frac{3N}{2^{2N}-1}\left(2^{2n-3}+2^{2N-2n-1}\right)\Gamma_{\rm av}\ . \tag{7}$$

4.1 Performance of BPSK-EDMA

Exploiting the tree structure of the overall PAM in Fig. 3, average-user BER may be directly computed as

$$P_{e,\rm av} \approx \frac{2^{N+1}-(N+2)}{N2^N}\operatorname{erfc}\left(\sqrt{\frac{3N}{2^{2N}-1}\Gamma_{\rm av}}\right)\ , \tag{8}$$

where $\operatorname{erfc}(x)=\frac{2}{\sqrt{\pi}}\int_x^{+\infty}\exp(-t^2)dt$. The derivation is shown in App. A.

Exact single-user BER may be evaluated along the same lines of [21], e.g. the error probability of the farthest and the nearest users,[2] denoted respectively $P_e(1)$ and $P_e(N)$, are found to be

$$P_e(1) = \frac{1}{2^N}\sum_{n=1}^{2^N-1}(-1)^{n-1}(2^N-n)\operatorname{erfc}\left(\sqrt{\frac{3N(2n-1)^2}{2^{2N}-1}\Gamma_{\rm av}}\right)\ ,$$

$$P_e(N) = \frac{1}{2^N}\sum_{n=1}^{2^{N-1}}\operatorname{erfc}\left(\sqrt{\frac{3N(2n-1)^2}{2^{2N}-1}\Gamma_{\rm av}}\right)\ .$$

However, exploiting the tree structure of the overall PAM in Fig. 3, a closed-form approximate expression for the single-user BER is easily found to be

$$P_e(n) \approx \frac{2^{N-n+1}-1}{2^N}\operatorname{erfc}\left(\sqrt{\frac{3N}{2^{2N}-1}\Gamma_{\rm av}}\right)\ . \tag{9}$$

The derivation is shown in App. B. Equations (6) and (9) provide the single-user BER w.r.t user SNR

$$P_e(n) \approx \frac{2^{N-n+1}-1}{2^N}\operatorname{erfc}\left(\sqrt{\frac{1}{2^{2(n-1)}}\Gamma_n}\right)\ . \tag{10}$$

4.2 Performance of QPSK-EDMA

Analogously to the case for BPSK modulation, average-user BER may be directly computed referring to the tree structure of the overall QAM shown in Fig. 4, obtaining

$$P_{e,\rm av} \approx \frac{s_q(N)}{2N2^{2N}}\operatorname{erfc}\left(\sqrt{\frac{3N}{2^{2N}-1}\Gamma_{\rm av}}\right)\ , \tag{11}$$

where

$$s_q(N) = \boldsymbol{u}(N)^T\boldsymbol{c}(2N)+\boldsymbol{v}(N)^T\left(\boldsymbol{c}(N)\otimes\mathbf{1}_{2^N}\right)\ ,$$

$$\boldsymbol{u}(N) = \left(\mathbf{1}^T_{2^N-2}, 0, 0, (\mathbf{1}^T_{2^N-1}, 0)\otimes\mathbf{1}^T_{2^N-2}, \mathbf{1}^T_{2^N-2}\right)^T\ ,$$

$$\boldsymbol{v}(N) = \left(\mathbf{1}^T_{2^N(2^N-2)}, 0, \mathbf{1}^T_{2^N-2}, 0\right)^T\ .$$

[2] It is worth noticing that farthest and nearest refer to the signal level, not to the physical distance.

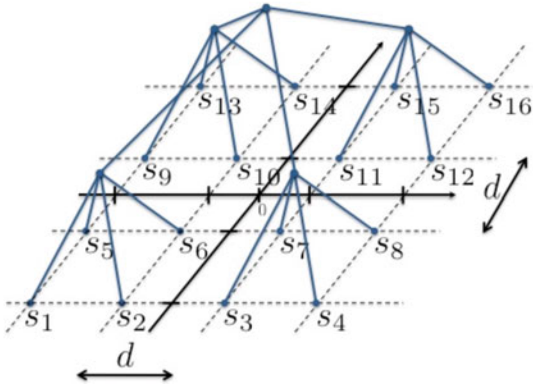

Fig. 4 Tree structure for a QPSK-EDMA system with 2 users

The derivation is shown in App. C.

Again, exploiting the tree structure of the overall QAM shown in Fig. 4, closed-form approximate expression for the single-user BER is found to be the same as in Eq. (9). The derivation is shown in App. D. Analogously the single-user BER w.r.t user SNR are the same as in Eq. (10).

4.3 Performance of RPSK-EDMA

The overall QAM constellation for the RPSK-EDMA is the same of the QPSK-EDMA. The only difference is that QAM symbols are mapped differently to the user bits, as shown in Fig. 5. Average-user BER is the same as for QPSK-EDMA, expressed by Eq. (11).

Closed-form approximate expression for the single-user BER w.r.t. average SNR is found as

$$P_e(n) \approx \frac{2^{N-n} + 2^{n-1} - 1}{2^N} \mathrm{erfc}\left(\sqrt{\frac{3N}{2^{2N} - 1}\Gamma_{\mathrm{av}}}\right), \tag{12}$$

The derivation is shown in App. E. Equations (7) and (12) provide the single-user BER w.r.t user SNR

$$P_e(n) \approx \frac{2^{N-n} + 2^{n-1} - 1}{2^N} \mathrm{erfc}\left(\sqrt{\frac{1}{2^{2n-3} + 2^{2N-2n-1}}\Gamma_n}\right). \tag{13}$$

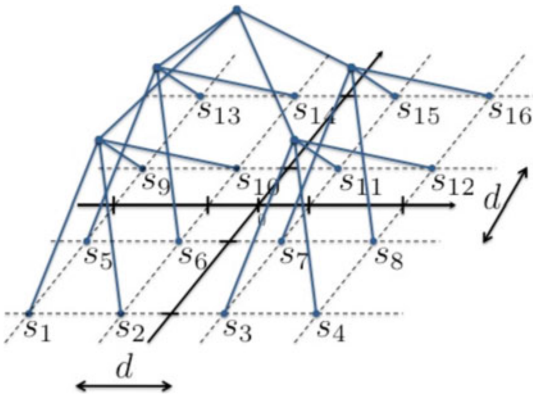

Fig. 5 Tree structure for a RPSK-EDMA system with 2 users

5 Comparison

System performance have been verified via computer simulations using the software MATLAB for QPSK-EDMA and RPSK-EDMA (being performance of BPSK-EDMA equal to the performance of QPSK-EDMA). Analytical and numerical results, for systems with 2 and 3 users, have shown excellent agreement: in order to save space we omit figures comparing analytical and numerical performance.

Figures 6 and 7 show the performance of the single user w.r.t. average SNR and user SNR, for systems with $N = 2$ (plotted with blue lines) and $N = 3$ users (plotted with red lines). In the 2-user case, the first user and the second user are represented with x-marks ($\times$) and plus ($+$), respectively. In the 3-user case, the first user is represented with diamonds ($\Diamond$), the second user with squares ($\Box$), and the third user with circles ($\circ$). As comparison term, in black with dotted line and asterisks ($*$), both figures show the performance of a system with arbitrary number of users adopting classical TDMA for channel sharing with QPSK modulation; such a system has the same performance of an EDMA system with $N = 1$ user.

More specifically, Fig. 6 is obtained with use of Eqs. (9) and (12). It is apparent how the average performance of the system degrades with the number of users almost 4 dB per additional user for limited number of users N, while asymptotic (with very large number of users N) loss is almost 6 dB, obtained via Eq. (11) as $\lim_{N\to\infty} \frac{3N(2^{2(N+1)}-1)}{3(N+1)2^{2N}-1}$, neglecting the coefficient $\frac{s_q(N)}{2N2^{2N}}$. Also, it is apparent how the performance of each user in the RPSK-EDMA case are close to the average performance of the system, while in the QPSK-EDMA case they are more spread although achieving the same average performance, i.e. RPSK-EDMA improves fairness w.r.t. QPSK-EDMA as expected.

Figure 7 is obtained with use of Eqs. (10) and (13) and shows several aspects. Firstly, referring to the QPSK-EDMA case, it is apparent how the performance of the first user are practically the same independently of the number of users N. Furthermore, it is apparent how the $(n + 1)$th user is almost 6 dB away from the nth user, also obtained comparing Γ_n and Γ_{n+1} in Eq. (10) and neglecting the coefficient $\frac{2^{N-n+1}-1}{2^N}$. In other words, an additional user willing to enter the system needs to pay a big price to make EDMA work, i.e. entering a system with N user he spends $6N$ dB more than the case in which he is transmitting alone. Secondly, referring to the RPSK-EDMA case, again it is apparent how fairness is improved having user performance more similar each other than in the QPSK-EDMA case.

It is worth noticing that in an RPSK-EDMA system with $N = 2$ users, both first and second users have equal performance. Also, such performance matches the average-user performance of the corresponding QPSK-EDMA system. Analogously, in an RPSK-EDMA system with $N = 3$ users, both first and third users have equal performance, while the second user has the same performance as the second user of the corresponding QPSK-EDMA system (again matching the average-user performance).

In order to evaluate the effective advantage of using EDMA, we have compared the normalized throughput η of systems using QPSK-EDMA, RPSK-EDMA with a system using TDMA with QPSK modulation. Similarly to [22], assuming that each user transmit packets containing L symbols, the normalized throughput of the overall system is computed as

$$\eta = \sum_{n=1}^{N} 2(1 - P_e(n))^L \ ,$$

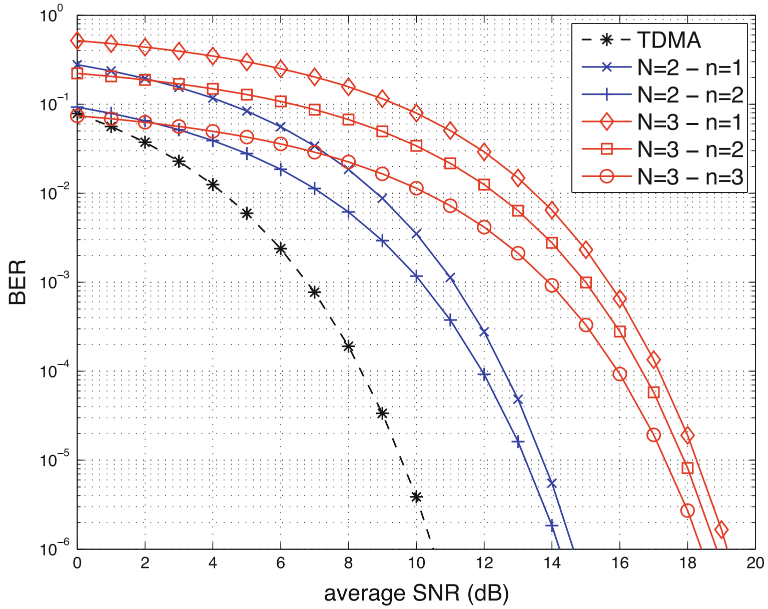

(a) QPSK case

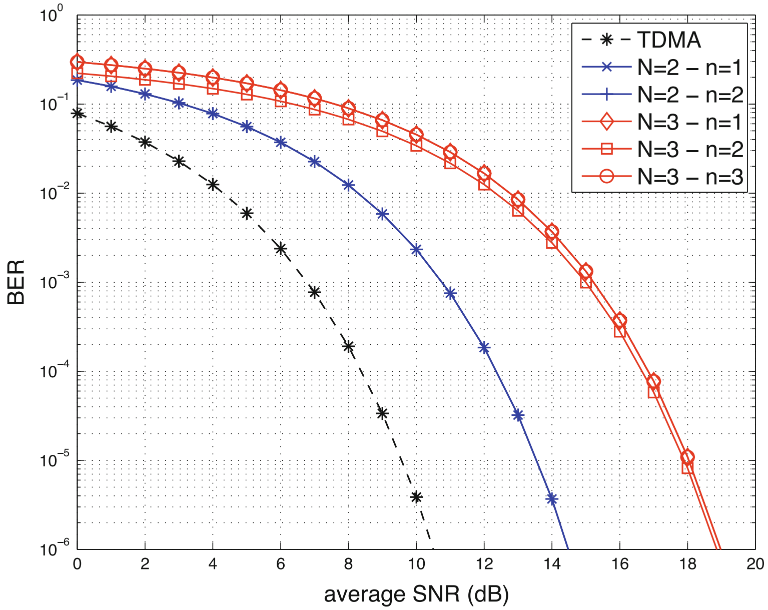

(b) RPSK case

Fig. 6 BER performance w.r.t. average SNR. EDMA systems with $N = 2$ and $N = 3$ users compared to TDMA

and plotted in Fig. 8 w.r.t. average SNR for $L = 100$. It is apparent how for large SNR it is better from the overall system point of view to have more users sharing the same time-frequency-code resource via QPSK-EDMA (the larger SNR, the more users),

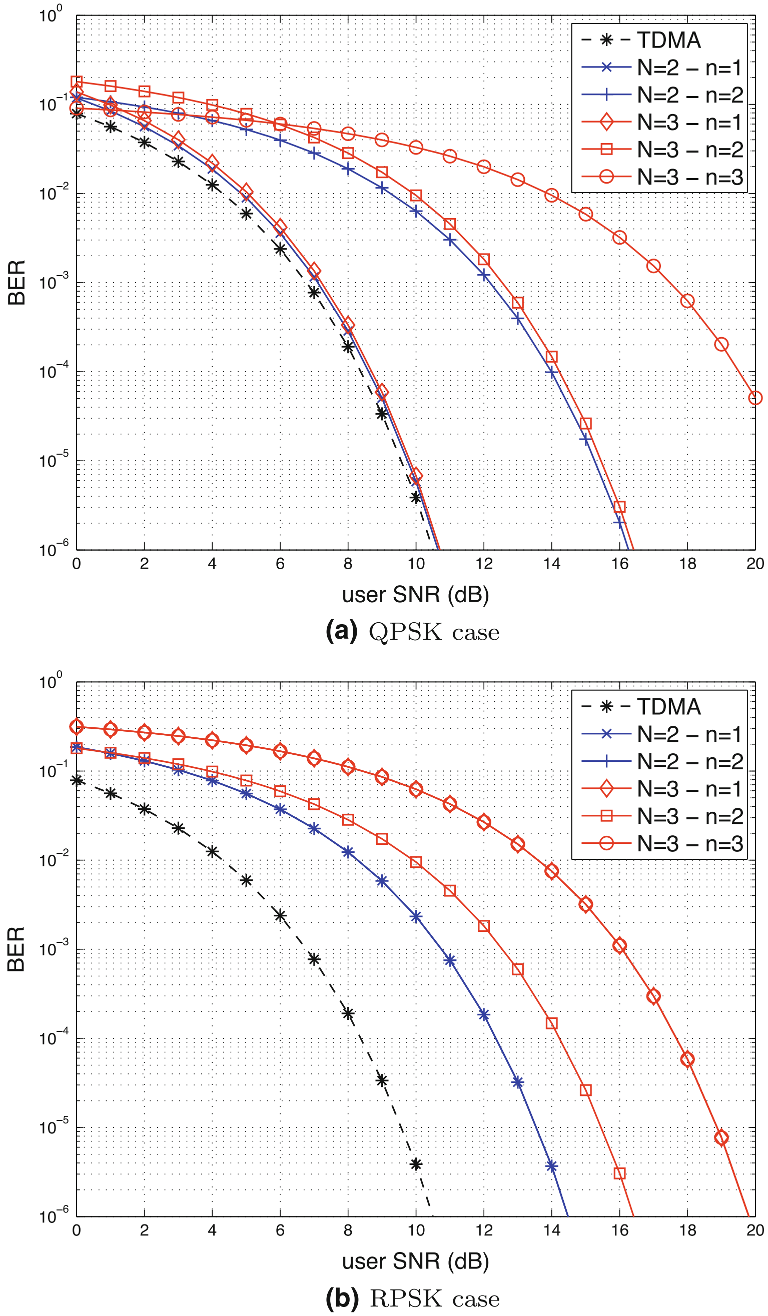

(a) QPSK case

(b) RPSK case

Fig. 7 BER performance w.r.t. user SNR. EDMA systems with $N = 2$ and $N = 3$ users compared to TDMA

and also how RPSK-EDMA preserves fairness issues with negligible degradation. More specifically, if the SNR is large enough, EDMA with N users allows to increase N times the normalized throughput w.r.t. to classical TDMA. On the other hand we must say that

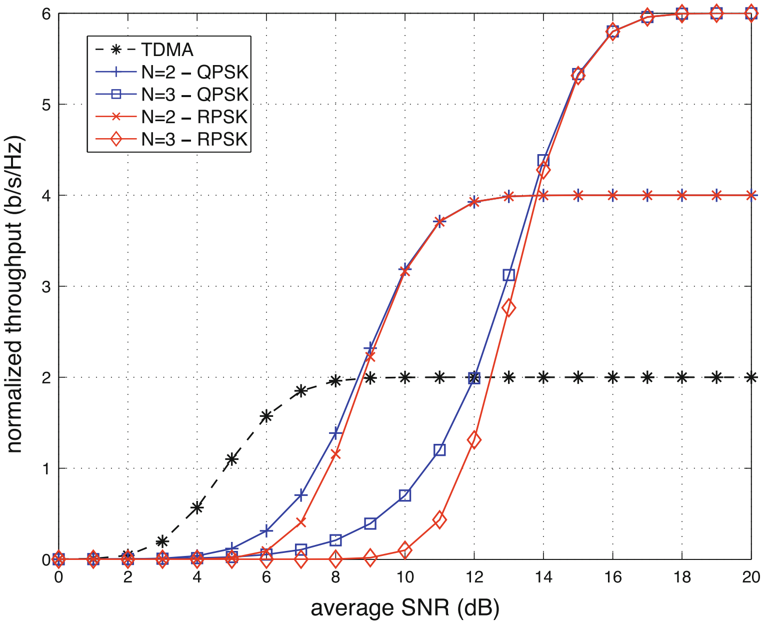

Fig. 8 Performance comparison in terms of normalized throughput. EDMA systems with $N = 2$ and $N = 3$ users compared to TDMA

EDMA may be used when users do not have energy constraints, alternatively practical energy constraints may limit the number of users employing EDMA. Also, it is worth noticing that RPSK-EDMA increases system fairness for a short-time range, however in a long-time range users will experience different battery lives (as for BPSK-EDMA and QPSK-EDMA), thus periodic rotation of the signal levels may be required. Furthermore, the receiver could select the number of users to detect depending on the signal levels, resulting in a system with variable "resolution" (with resolution related to detectable users).

Finally, we would like to point out that: (i) in a flat-fading environment the structure of the constellation would be destroyed thus the proposed scheme may appear useless, however (in slow fading environments) channel state information may be available both at transmitter and receiver sides, thus the transmitter side could employ channel inversion in order to compensate for the distortion of the constellation and obtain a regular constellation at receiver location; (ii) in a frequency-selective fading environment, OFDM can be considered to change the dispersive channel into several flat-fading subchannels, and then EDMA may be directly applied on each subcarrier. It is worth noticing that assuming a system with M subcarrier, then Eq. (1) will change into

$$y^{(m)} = \sum_{n=1}^{N} g_n^{(m)} x_n^{(m)} + w^{(m)} = \sum_{n=1}^{N} h_n^{(m)} \sqrt{\mathcal{E}_n^{(m)}} x_n^{(m)} + w^{(m)} , \quad m = 1, \ldots, M ,$$

with obvious meaning of the notation. It is apparent how the presence of both the channel coefficients and the multiple subcarriers introduce the possibility of resource optimization while preserving fairness issues, however the effects of fading on the performance of the system is left for future work.

6 Conclusion

Multiple access on the same band and with the same pulse is feasible with low-complexity reception schemes, using successive decoding, if users magnitudes are properly chosen. Conditions on magnitudes are derived in order to separate each user, revealing its contribution from the aggregate received symbol. Performance of such a scheme, denoted EDMA, has been derived for uncoded transmission over AWGN channels, both in terms of BER and normalized throughput. Multi-user systems in which each user employs BPSK, QPSK and RPSK modulation has been considered, showing performance from the point of view of both the system and the single user. Large gains in terms of normalized throughput are achieved in large SNR regime in comparison to classical TDMA.

A Average-User Performance of BPSK-EDMA

In order to have compact notation, we define the following integrals

$$\begin{aligned}
q_{(1)} &= \Pr(\mathcal{N}(0,\sigma^2) < d/2) \\
&= 1 - \frac{1}{2}\operatorname{erfc}\left(\sqrt{\frac{3N}{2^{2N}-1}\Gamma_{\text{av}}}\right) , \\
q_{(2)} &= \Pr(|\mathcal{N}(0,\sigma^2)| < d/2) \\
&= 1 - \operatorname{erfc}\left(\sqrt{\frac{3N}{2^{2N}-1}\Gamma_{\text{av}}}\right) , \\
q_{(3)} &= \Pr(|\mathcal{N}(0,\sigma^2) - d| < d/2) \\
&= \frac{1}{2}\operatorname{erfc}\left(\sqrt{\frac{3N}{2^{2N}-1}\Gamma_{\text{av}}}\right) - \frac{1}{2}\operatorname{erfc}\left(\sqrt{\frac{27N}{2^{2N}-1}\Gamma_{\text{av}}}\right) , \\
q_{(4)} &= \Pr(\mathcal{N}(0,\sigma^2) > d/2) \\
&= 1 - q_{(1)} ,
\end{aligned}$$

The code induced by the gains defined in Eq. (5) has a tree structure with the farthest user corresponding to the least significant bit, as shown in Fig. 3. Assuming uniform *a priori* probabilities, we have

$$P_{e,\text{av}} = \frac{1}{N}\frac{1}{2^N}\sum_{i=1}^{2^N}\sum_{j=1}^{2^N} P_{i,j}E_{i,j} , \tag{14}$$

where $P_{i,j}$ (entry of the *channel matrix* $\boldsymbol{P}$) represents the probability that the symbol s_j of the overall PAM is received when the symbol s_i has been transmitted; and $E_{i,j}$ (entry of the *bit-error matrix* $\boldsymbol{E}$) is the corresponding number of bits in error. Under the assumption that the errors only occur between adjacent symbols on the overall PAM (large SNR approximation), the channel matrix $\boldsymbol{P}$ can be approximated with a $2^N \times 2^N$ tri-diagonal matrix. All entries of $\boldsymbol{P}$ are null with exception of $\boldsymbol{p}(0) = \text{diag}(\boldsymbol{P}, 0)$, $\boldsymbol{p}(1) = \text{diag}(\boldsymbol{P}, 1)$, $\boldsymbol{p}(-1) = \text{diag}(\boldsymbol{P}, -1)$, thus Eq. (14) becomes

$$P_{e,\text{av}} \approx \frac{\left(\boldsymbol{e}(0)^T\boldsymbol{p}(0) + \boldsymbol{e}(1)^T\boldsymbol{p}(1) + \boldsymbol{e}(-1)^T\boldsymbol{p}(-1)\right)}{N2^N} , \tag{15}$$

where $\boldsymbol{e}(0) = \mathrm{diag}(\boldsymbol{E}, 0)$, $\boldsymbol{e}(1) = \mathrm{diag}(\boldsymbol{E}, 1)$, $\boldsymbol{e}(-1) = \mathrm{diag}(\boldsymbol{E}, -1)$. Closer view of the tree structure of the overall PAM in Fig. 3 easily shows that

$$\begin{cases} \boldsymbol{p}(0) = \left(q_{(1)}, q_{(2)}\mathbf{1}^T_{2^N-2}, q_{(1)}\right)^T \\ \boldsymbol{p}(1) = \left(q_{(3)}\mathbf{1}^T_{2^N-2}, q_{(1)}\right)^T \\ \boldsymbol{p}(-1) = \boldsymbol{I}^{(\mathrm{a})}_{2^N-1}\boldsymbol{p}(1) \end{cases}, \qquad \begin{cases} \boldsymbol{e}(0) = \mathbf{0}_{2^N} \\ \boldsymbol{e}(1) = \boldsymbol{c}(N) \\ \boldsymbol{e}(-1) = \boldsymbol{c}(N) \end{cases},$$

where $\boldsymbol{c}(N)$ may be computed inductively as $\boldsymbol{c}(n) = \left(\boldsymbol{c}(n-1)^T, n, \boldsymbol{c}(n-1)^T\right)^T$ with $\boldsymbol{c}(1) = 1$, see also [14, 15]. Finally, replacing the corresponding expressions for the vectors in Eq. (15), we obtain

$$P_{e,\mathrm{av}} \approx \frac{1}{N}\frac{1}{2^{N-1}}\left(q_{(3)}\mathbf{1}^T_{2^N-2}, q_{(4)}\right)\boldsymbol{c}(N) ,$$

and noticing that $\mathbf{1}^T_{2^N-1}\boldsymbol{c}(N) = 2^{N+1} - (N+2)$, then Eq. (8).

B Single-User Performance of BPSK-EDMA

Due to the symmetry of the overall PAM constellation, the performance of the nth user may be evaluated as the conditional probability of the nth user being in error given that it has transmitted the bit 0. Denote $\mathcal{S}_0(n)$ and $\mathcal{S}_0^{(c)}(n)$ the subset of the symbols corresponding to 0 transmission by the nth user and the subset of the remaining symbols, respectively. Assuming uniform *a priori* probabilities and noticing that $|\mathcal{S}_0(n)| = 2^{N-1}$, we have

$$P_e(n) = \frac{1}{2^{N-1}}\sum_{s\in\mathcal{S}_0(n),\ \hat{s}\in\mathcal{S}_0^{(c)}(n)} \Pr(s, \hat{s}) ,$$

where $\hat{s}$ denote the decoded symbol. Under large SNR approximation, we can assume again that errors happen only between adjacent symbols. It is worth noticing that $\frac{1}{2}\mathrm{erfc}\left(\sqrt{\frac{d^2}{8\sigma^2}}\right)$ represents the dominant term for the probability of confusing two adjacent symbols whose distance is d when noise variance is σ^2, irrespectively if they are inner symbols or not. Denoting $\mathcal{D}(n) = \left\{(s, \hat{s}) \in \mathcal{S}_0(n) \times \mathcal{S}_0^{(c)}(n) : \ s \text{ and } \hat{s} \text{ are adjacent}\right\}$, we only need to count the number of elements in $\mathcal{D}$, thus denoting $\ell_{\mathcal{D}}(n) = |\mathcal{D}(n)|$ we have

$$P_e(n) \approx \frac{\ell_{\mathcal{D}}(n)}{2^N}\mathrm{erfc}\left(\sqrt{\frac{d^2}{8\sigma^2}}\right) .$$

Simple inspection of the sets $\mathcal{S}_0(n)$ and $\mathcal{S}_0^{(c)}(n)$, depicted in Fig. 9 for a system with 3 users, shows that $\ell_{\mathcal{D}}(n) = 2^{N-n+1} - 1$, finally having Eq. (9).

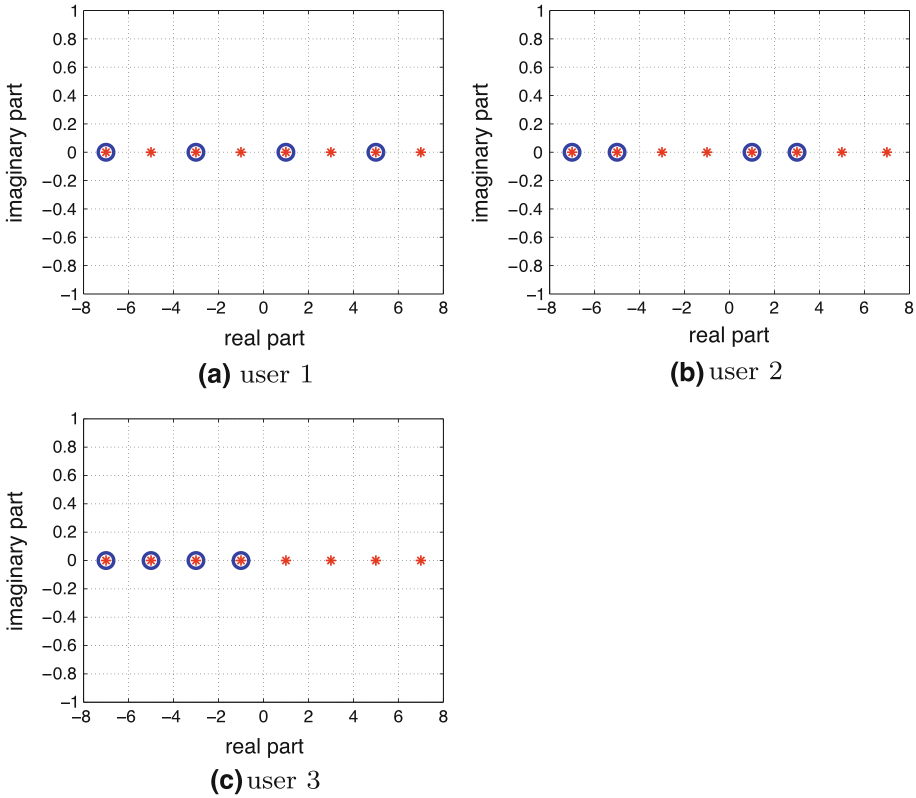

Fig. 9 Signal constellation for 3-user BPSK-EDMA. *Red asterisks* represent all the constellation, *blue circles* represent the symbols belonging to $\mathcal{S}_0(n)$

C Average-User Performance of QPSK-EDMA

In order to have compact notation, we define the following integrals

$$\begin{aligned}
q_{\mathrm{Co}} &= \Pr(\Re(\mathcal{N}_{\mathbb{C}}(\mathbf{0}_2, \sigma^2 \boldsymbol{I}_2)) > d/2, \Im(\mathcal{N}_{\mathbb{C}}(\mathbf{0}_2, \sigma^2 \boldsymbol{I}_2)) > d/2) \\
&= q_{(4)}^2 \ , \\
q_{\mathrm{Lh}} &= \Pr(\Re(\mathcal{N}_{\mathbb{C}}(\mathbf{0}_2, \sigma^2 \boldsymbol{I}_2)) < d/2, |\Im(\mathcal{N}_{\mathbb{C}}(\mathbf{0}_2, \sigma^2 \boldsymbol{I}_2)) - d| < d/2) \\
&= q_{(1)} q_{(3)} \ , \\
q_{\mathrm{Lp}} &= \Pr(|\Re(\mathcal{N}_{\mathbb{C}}(\mathbf{0}_2, \sigma^2 \boldsymbol{I}_2))| < d/2, \Im(\mathcal{N}_{\mathbb{C}}(\mathbf{0}_2, \sigma^2 \boldsymbol{I}_2)) > d/2) \\
&= q_{(2)} q_{(4)} \ , \\
q_{\mathrm{In}} &= \Pr(|\Re(\mathcal{N}_{\mathbb{C}}(\mathbf{0}_2, \sigma^2 \boldsymbol{I}_2))| < d/2, |\Im(\mathcal{N}_{\mathbb{C}}(\mathbf{0}_2, \sigma^2 \boldsymbol{I}_2)) - d| < d/2) \\
&= q_{(2)} q_{(3)} \ .
\end{aligned}$$

Analogously to the case for BPSK modulation, referring to the tree structure in Fig. 4, assuming uniform *a priori* probabilities, we have

$$P_{e,\mathrm{av}} = \frac{1}{2N} \frac{1}{2^{2N}} \sum_{i=1}^{2^{2N}} \sum_{j=1}^{2^{2N}} P_{i,j} E_{i,j} \ , \tag{16}$$

with analogous meaning for $P_{i,j}$ and $E_{i,j}$. Again we assume that errors only occur between adjacent symbols on the overall QAM (large SNR approximation), thus the channel matrix $\boldsymbol{P}$ can be approximated with a $2^{2N} \times 2^{2N}$ matrix with 5 diagonals containing non-zero entries: $\boldsymbol{p}(0) = \mathrm{diag}(\boldsymbol{P}, 0)$, $\boldsymbol{p}(1) = \mathrm{diag}(\boldsymbol{P}, 1)$, $\boldsymbol{p}(2^N) = \mathrm{diag}(\boldsymbol{P}, 2^N)$, $\boldsymbol{p}(-1) = \mathrm{diag}(\boldsymbol{P}, -1)$, $\boldsymbol{p}(-2^N) = \mathrm{diag}(\boldsymbol{P}, -2^N)$, thus Eq. (16) becomes

$$\begin{aligned} P_{e,\mathrm{av}} = \frac{1}{2N}\frac{1}{2^{2N}} \Big(& \boldsymbol{e}(0)^T \boldsymbol{p}(0) + \boldsymbol{e}(1)^T \boldsymbol{p}(1) + \boldsymbol{e}(2^N)^T \boldsymbol{p}(2^N) \\ & + \boldsymbol{e}(-1)^T \boldsymbol{p}(-1) + \boldsymbol{e}(-2^N)^T \boldsymbol{p}(-2^N) \Big) \ , \end{aligned} \tag{17}$$

where

$$\begin{aligned} \boldsymbol{e}(0) &= \mathrm{diag}(\boldsymbol{E}, 0) \ , \\ \boldsymbol{e}(1) &= \mathrm{diag}(\boldsymbol{E}, 1) \ , \\ \boldsymbol{e}(2^N) &= \mathrm{diag}(\boldsymbol{E}, 2^N) \ , \\ \boldsymbol{e}(-1) &= \mathrm{diag}(\boldsymbol{E}, -1) \ , \\ \boldsymbol{e}(-2^N) &= \mathrm{diag}(\boldsymbol{E}, -2^N) \ . \end{aligned}$$

Closer view of the tree structure of the overall QAM easily shows that

$$\begin{aligned} \boldsymbol{p}(0) &= \left(\boldsymbol{p}_{(1)}^T(0), \boldsymbol{p}_{(2)}^T(0), \ldots, \boldsymbol{p}_{(2^N)}^T(1)\right)^T \ , \\ \boldsymbol{p}(1) &= \left(\boldsymbol{p}_{(1)}^T(1), \boldsymbol{p}_{(2)}^T(1), \ldots, \boldsymbol{p}_{(2^N)}^T(1)\right)^T \ , \\ \boldsymbol{p}(2^N) &= \left(\boldsymbol{p}_{(1)}^T(2^N), \boldsymbol{p}_{(2)}^T(2^N), \ldots, \boldsymbol{p}_{(2^N-1)}^T(2^N)\right)^T \ , \\ \boldsymbol{p}(-1) &= \boldsymbol{I}_{2^{2N}-1}^{(\mathrm{a})} \boldsymbol{p}(1) \ , \\ \boldsymbol{p}(-2^N) &= \boldsymbol{I}_{2^{2N}-2^N}^{(\mathrm{a})} \boldsymbol{p}(2^N) \ , \end{aligned}$$

and

$$\begin{aligned} \boldsymbol{e}(0) &= \boldsymbol{0}_{2^{2N}} \ , \\ \boldsymbol{e}(1) &= \boldsymbol{c}(2N) \ , \\ \boldsymbol{e}(2^N) &= \boldsymbol{c}(N) \otimes \boldsymbol{1}_{2^N} \ , \\ \boldsymbol{e}(-1) &= \boldsymbol{c}(2N) \ , \\ \boldsymbol{e}(-2^N) &= \boldsymbol{c}(N) \otimes \boldsymbol{1}_{2^N} \ , \end{aligned}$$

where

$$\boldsymbol{p}_{(n)}^T(0) = \begin{cases} \left(q_{(1)}^2, q_{(1)}q_{(2)}\boldsymbol{1}_{2^N-2}^T, q_{(1)}^2\right) & n = 1 \\ \left(q_{(1)}q_{(2)}, q_{(2)}^2\boldsymbol{1}_{2^N-2}^T, q_{(1)}q_{(2)}\right) & n = 2, \ldots, 2^N - 1 \\ \left(q_{(1)}^2, q_{(1)}q_{(2)}\boldsymbol{1}_{2^N-2}^T, q_{(1)}^2\right) & n = 2^N \end{cases}$$

$$\boldsymbol{p}_{(n)}^T(1) = \begin{cases} \left(q_{\mathrm{Lh}}\boldsymbol{1}_{2^N-2}^T, q_{\mathrm{Co}}, 0\right) & n = 1 \\ \left(q_{\mathrm{In}}\boldsymbol{1}_{2^N-2}^T, q_{\mathrm{Lp}}, 0\right) & n = 2, \ldots, 2^N - 1 \\ \left(q_{\mathrm{Lh}}\boldsymbol{1}_{2^N-2}^T, q_{\mathrm{Co}}\right) & n = 2^N \end{cases}$$

$$\boldsymbol{p}_{(n)}^T(2^N) = \begin{cases} \left(q_{\mathrm{Lh}}, q_{\mathrm{In}}\mathbf{1}_{2^N-2}^T, q_{\mathrm{Lh}}\right) & n = 1, \ldots, 2^N - 2 \\ \left(q_{\mathrm{Co}}, q_{\mathrm{Lp}}\mathbf{1}_{2^N-2}^T, q_{\mathrm{Co}}\right) & n = 2^N - 1 \end{cases}$$

Finally, replacing the corresponding expressions for the vectors in Eq. (17), we obtain

$$P_{e,\mathrm{av}} \approx \frac{\left(\boldsymbol{p}(1)^T\boldsymbol{c}(2N) + \boldsymbol{p}(2^N)^T(\boldsymbol{c}(N) \otimes \mathbf{1}_{2^N})\right)}{2N2^{2N-1}},$$

and then Eq. (11).

D Single-User Performance of QPSK-EDMA

Again, due to the symmetry of the overall QAM constellation, the performance of the nth user may be evaluated as the conditional probability of the nth user being in error given that it has transmitted the bit couple 00. Denoting $\mathcal{S}_{00}(n)$ and $\mathcal{S}_{00}^{(c)}(n)$ the subset of the symbols corresponding to 00 transmission by the nth user and the subset of the remaining symbols,

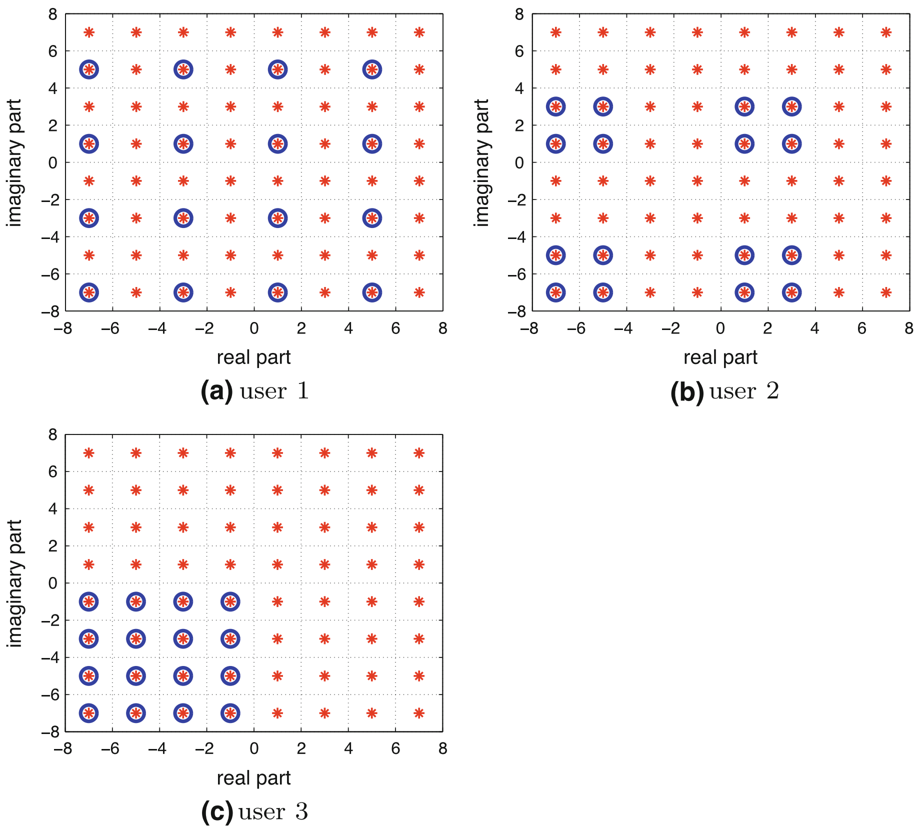

Fig. 10 Signal constellation for 3-user QPSK-EDMA. *Red asterisks* represent all the constellation, *blue circles* represent the symbols belonging to $\mathcal{S}_{00}(n)$

respectively, assuming uniform *a priori* probabilities, and being $|\mathcal{S}_{00}(n)| = 2^{2(N-1)}$, under large SNR approximation we have

$$P_e(n) \approx \frac{\ell_{\mathcal{D}}(n)}{2^{2N-1}} \text{erfc}\left(\sqrt{\frac{d^2}{8\sigma^2}}\right) ,$$

where $\mathcal{D}(n) = \left\{(s, \hat{s}) \in \mathcal{S}_{00}(n) \times \mathcal{S}_{00}^{(c)}(n) : \ s \text{ and } \hat{s} \text{ are adjacent}\right\}$, and $\ell_{\mathcal{D}}(n) = |\mathcal{D}(n)|$. Looking at the structure of the sets $\mathcal{S}_{00}(n)$ in Fig. 10, we can divide each set in 3 subsets: $\mathcal{T}_1$ one containing the cluster of symbols on the left-lower corner, having adjacent symbols only on 2 sides (up and right); $\mathcal{T}_2$ containing the clusters of symbols on the left side and on the lower side, having adjacent symbols on 3 sides (up, down, and right; up, left, and right); $\mathcal{T}_3$ containing the remaining clusters of symbols, having adjacent symbols on 4 sides (up, down, left, and right). Then, we compute $\ell_{\mathcal{D}}(n) = \alpha(n)a(n) + \beta(n)b(n) + \gamma(n)c(n)$, where: $\alpha(n)$, $\beta(n)$, and $\gamma(n)$ are the number of symbols belonging to $\mathcal{S}_{00}^{(c)}(n)$ and adjacent to the single cluster in $\mathcal{T}_1$, $\mathcal{T}_2$, and $\mathcal{T}_3$, respectively; $a(n)$, $b(n)$, and $c(n)$ are the number of clusters in $\mathcal{T}_1$, $\mathcal{T}_2$, $\mathcal{T}_3$, respectively. Inspection of Fig. 10 shows that $\alpha(n) = 2 \cdot 2^{n-1}$, $\beta(n) = 3 \cdot 2^{n-1}$, $\gamma(n) = 4 \cdot 2^{n-1}$, and also $a(n) = 1$, $b(n) = 2 \cdot (2^{N-n} - 1)$, $c(n) = 2^{2(N-n)} - 2 \cdot 2^{N-n} + 1$, from which $\ell_{\mathcal{D}}(n) = 2^{2N-n} - 2^{N-1}$, and then Eq. 9.

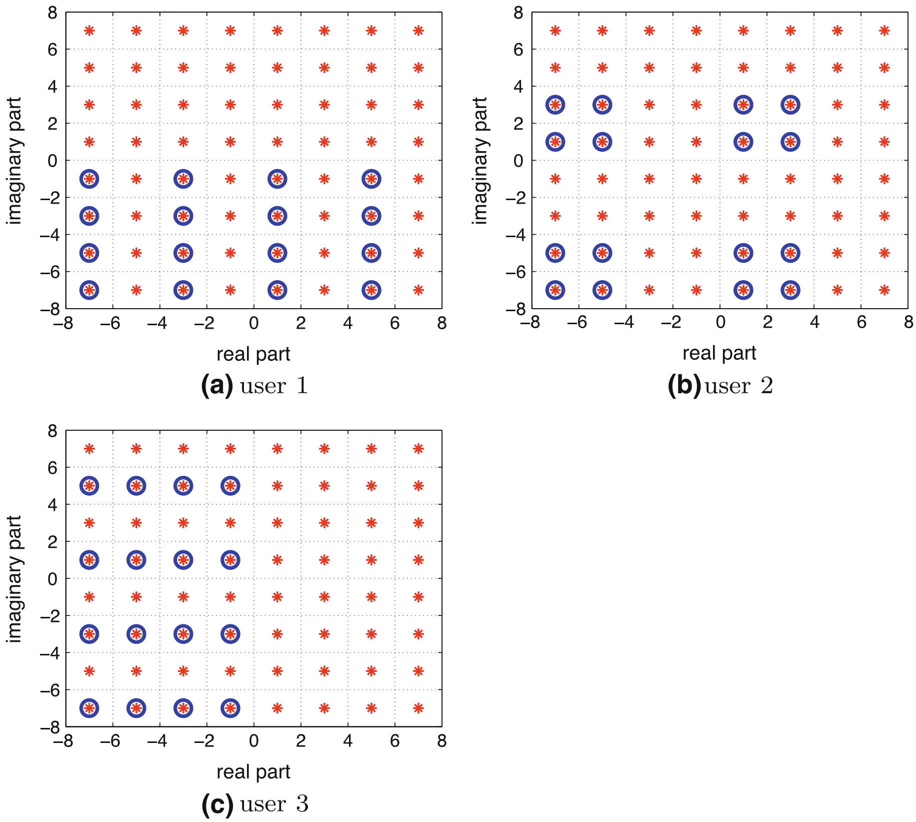

Fig. 11 Signal constellation for 3-user RPSK-EDMA. *Red asterisks* represent all the constellation, *blue circles* represent the symbols belonging to $\mathcal{S}_{00}(n)$

E Single-User Performance of RPSK-EDMA

Again, due to the symmetry of the overall QAM constellation, the performance of the nth user may be evaluated as the conditional probability of the nth user being in error given that it has transmitted the bit couple 00. Denoting $\mathcal{S}_{00}(n)$ and $\mathcal{S}_{00}^{(c)}(n)$ the subset of the symbols corresponding to 00 transmission by the nth user and the subset of the remaining symbols, respectively, assuming uniform *a priori* probabilities, and being $|\mathcal{S}_{00}(n)| = 2^{2(N-1)}$, under large SNR approximation we have

$$P_e(n) \approx \frac{\ell_{\mathcal{D}}(n)}{2^{2N-1}} \operatorname{erfc}\left(\sqrt{\frac{d^2}{8\sigma^2}}\right) ,$$

where $\mathcal{D}(n) = \left\{(s, \hat{s}) \in \mathcal{S}_{00}(n) \times \mathcal{S}_{00}^{(c)}(n) : \; s \text{ and } \hat{s} \text{ are adjacent}\right\}$, and $\ell_{\mathcal{D}}(n) = |\mathcal{D}(n)|$. Looking at the structure of the sets $\mathcal{S}_{00}(n)$ in Fig. 11, we can compute $\ell_{\mathcal{D}}(n) = N^{(v)}(n) + N^{(h)}(n)$, where $N^{(h)}(n)$ and $N^{(h)}(n)$ are the numbers of neighbors from $\mathcal{S}_{00}(n)$ and $\mathcal{S}_{00}^{(c)}(n)$ with vertical and horizontal alignment, respectively. Inspection of Fig. 11 shows that $N^{(v)}(n) = 2^{N-1}(2^n - 1)$ and $N^{(h)}(n) = 2^{N-1}(2^{N-n+1} - 1)$, from which $\ell_{\mathcal{D}}(n) = 2^{N-n} + 2^{n-1} - 1$, thus Eq. 12.

References

1. Haykin, S. (2000). *Digital Communications*. West Sussex, U.K.: Wiley.
2. Proakis, J. G. (2000). *Digital Communications*. New York: McGraw Hill.
3. Rappaport, T. F. (2002). *Wireless Communications: Principles and Practice*. Prentice: Prentice Hall.
4. Verdú, S. (1998). *Multiuser Detection*. Cambridge: Cambridge University Press.
5. Guess, T., & Varanasi, M. K. (2003). Signal design for bandwidth-efficient multiple-access communications based on eigenvalue optimization. *IEEE Transactions on Information Theory, 46*(6), 2045–2058.
6. Varanasi, M. K., & Guess, T. (2001). Bandwidth-efficient multiple access (BEMA): A new strategy based on signal design under quality-of-service constraints for successive-decoding-type multiuser receivers. *IEEE Transactions on Communications, 49*(5), 844–854.
7. Viswanath, P., Anantharam, V., & Tse, D. N. C. (1999). Optimal sequences, power control, and user capacity of synchronous CDMA systems with linear MMSE multiuser receivers. *IEEE Transactions on Information Theory, 45*(6), 1968–1983.
8. Guess, T., & Varanasi, M. K. (2003). A Comparison of bandwidth-efficient multiple access to other signal designs for correlated waveform multiple-access communications. *IEEE Transactions on Information Theory, 49*(6), 1558–1564.
9. Gilhousen, K. S., Jacobs, I. M., Padovani, R., Viterbi, A. J., Weaver, L. A., & Wheatley, C. E. (1991). On the capacity of a cellular CDMA system. *IEEE Transactions on Vehicular Technology, 40*(2), 303–311.
10. Zander, J. (1992). Performance of optimum transmitter power control in cellular radiosystems. *IEEE Transactions on Vehicular Technology, 41*(1), 57–62.
11. Aulin, T. M., & Espineira, R. (June 1999). Trellis coded multiple access (TCMA). *IEEE International Conference on Communications (ICC)*, (pp. 1177–1181).
12. Brannstrom, F. N., Aulin, T. M., & Rasmussen, L. K. (2001). Constellation-constrained capacity for trellis code multiple access systems. *IEEE Global Telecommunications Conference (GLOBECOM), 2*, 791–795.
13. Zhang, W., D'Amours, C., & Yongacoglu, A. (2004). Trellis coded modulation design for multi-user systems on AWGN channels. *IEEE Vehicular Technology Conference (VTC), 3*, 1722–1726.
14. Salvo Rossi, P., Romano, G., Mattera, D., Palmieri, F., & Marano, S. (July 2006). An energy-division multiple access scheme. *International conference on information fusion (ICIF)* (pp. 1–5).
15. Salvo Rossi, P., Romano, G., Mattera, D., Palmieri, F., & Marano, S. (March 2007). A scheme for multiuser communications based on energy division. *Conference on information sciences and systems (CISS)*, pp. 561–565.
16. Steele, R., & Hanzo, L. (1999). *Mobile radio communications, 2nd ed.* West Sussex, U.K.: Wiley.

17. Romano, G., Ciuonzo, D., Palmieri, F., & Salvo Rossi, P. (June 2007). Group gain design for overloaded CDMA. *IEEE international workshop on signal processing advances in wireless communications (SPAWC)*, pp. 1–5.
18. Romano, G., Palmieri, F., Willett, P. K., & Mattera, D. (March 2005). Separability and gain control for overloaded CDMA. *Conference on Information Sciences and Systems (CISS)*.
19. Verdú, S. (1986). Optimum multiuser asymptotic efficiency. *IEEE Transactions on Communications, 34*(9), 890–897.
20. Varanasi, M. K. (1999). Decision feedback multiuser detection: A systematic approach. *IEEE Transactions on Information Theory, 45*(1), 219–240.
21. Cho, K., & Yoon, D. (2002). On the general BER expression of one- and two-dimensional amplitude modulations. *IEEE Transactions on Communications, 50*(7), 1074–1080.
22. Stamoulis, A., & Al-Dhahir, N. (2003). Impact of space-time block codes on 802.11 network throughput. *IEEE Transactions on Wireless Communications, 2*(5), 1029–1039.

Author Biographies

Pierluigi Salvo Rossi was born in Naples, Italy, on April 26, 1977. He received the "Laurea" degree (summa cum laude) in Telecommunications Engineering and the Ph.D. in Computer Engineering, respectively in 2002 and in 2005, both from University of Naples "Federico II", Naples, Italy. During his Ph.D. studies, he has been at the CIRASS (Inter-departmental Research Center for Signals Analysis and Synthesis), University of Naples "Federico II", Naples, Italy; at the Department of Information Engineering, Second University of Naples, Aversa (CE), Italy; and visiting the CSPL (Communications and Signal Processing Laboratory), Department of Electrical and Computer Engineering, Drexel University, Philadelphia, PA, US. He was Adjunct Professor at the Department of Information Engineering, Second University of Naples, Aversa (CE), Italy. He worked as Postdoc at the Department of Computer Science and Systems, University of Naples "Federico II", Naples, Italy; at the Department of Information Engineering, Second University of Naples, Aversa (CE), Italy; at the Department of Electronics and Telecommunications, Norwegian University of Science and Technology, Trondheim, Norway; and visited the Department of Electrical and Information Technology, Lund University, Lund, Sweden. He is currently Assistant Professor in Telecommunications at the Department of Information Engineering, Second University of Naples, Aversa (CE), Italy. His research interests fall within the areas of signal processing and communications.

Gianmarco Romano received the Laurea degree in Electronic Engineering from the University of Naples "Federico II" and the Ph.D. degree from the Second University of Naples, in 2000 and 2004, respectively. From 2000 to 2002 he has been Researcher at the National Laboratory for Multimedia Communications (C.N.I.T.) in Naples, Italy. In 2003 he was Visiting Scholar at the Department of Electrical and Electronic Engineering, University of Conncticut, Storrs, USA. Since 2005 he has been with the Dipartimento di Ingegneria dell'Informazione, Seconda Università di Napoli, and in 2006 has been appointed Ricercatore (Assistant Professor). His research interests are in the area of signal processing for wireless multiple-input multiple-output (MIMO) and code division multiple access (CDMA) channels, multiple description coding (MDC), packet networks modelling.

Francesco Palmieri received his Laurea in Ingegneria Elettronica cum laude from Università degli Studi di Napoli Federico II, Italy, in 1980. In 1983, he was awarded a Fulbright scholarship to conduct graduate studies at the University of Delaware, Newark, where he received a M.S. degree in applied sciences and a Ph.D. in electrical engineering in 1985 and 1987, respectively. In 1981, he served as a 2nd Lieutenant in the Italian Army in fulfillment of draft duties. In 1982 and 1983, he was with the ITT firms: FACE SUD Selettronica in Salerno (currently Alcatel), Italy, and Bell Telephone Manufacturing Company in Antwerpen, Belgium, as a designer of digital telephone systems. He was appointed Assistant Professor in Electrical and Systems Engineering at the University of Connecticut, Storrs, in 1987, where he was awarded tenure and promotion to associate professor in 1993. In the same year, after a national competition, he was awarded the position of Professore Associato at the Dipartimento di Ingegneria Elettronica e delle Telecomunicazioni at Università degli Studi di Napoli Federico II, Italy, where he has been until October 2000. In February 2000, he was nominated Professore Ordinario di Telecomunicazioni after a national competition and appointed in November 2000 at Dipartimento di Ingegneria dell'Informazione, Seconda Università di Napoli, Aversa, Italy. His reaserch interests are in the areas of signal processing, communications, information theory and neural networks.